J. Membrane Biol. 168, 241–251 (1999)

The Journal of
Membrane
Biology

Sodium Recirculation and Isotonic Transport in Toad Small Intestine

S. Nedergaard, E.H. Larsen, H.H. Ussing
August Krogh Institute, The University of Copenhagen, Universitetsparken 13. DK-2100 Copenhagen Ø, Denmark

Received: 14 October 1998/Revised: 14 January 1999

Abstract. Isolated small intestine of toad (*Bufo bufo*) was mounted on glass tubes for perfusion studies with oxygenated amphibian Ringer's solution containing glucose and acetate. Under open-circuit conditions (V_t = −3.9 ± 1.8 mV, N = 14) the preparation generated a net influx of $^{134}Cs^+$. The time course of unidirectional $^{134}Cs^+$-fluxes was mono-exponential with similar rate constants for influx and outflux when measured in the same preparation. The flux-ratio was time invariant from the beginning of appearance of the tracers to steady state was achieved. Thus, just a single pathway, the paracellular pathway, is available for transepithelial transport of Cs^+. From the ratio of unidirectional Cs^+-fluxes the paracellular force was calculated to be, 18.2 ± 1.5 mV (N = 6), which is directed against the small transepithelial potential difference. The paracellular netflux of cesium ions, therefore, is caused by solvent drag. The flux of $^{134}Cs^+$ entering and trapped by the cells was of a magnitude similar to that passing the paracellular route. Therefore, independent of the convective flux of $^{134}Cs^+$, every second $^{134}Cs^+$ ion flowing into the lateral space was pumped into the cells rather than proceeding, via the low resistance pathway, to the serosal bath. It is thus indicated that the paracellular convective flow of $^{134}Cs^+$ is driven by lateral Na^+/K^+-pumps. Transepithelial unidirectional $^{42}K^+$ fluxes did not reach steady state within an observation period of 70 min, indicating that components of the fluxes in both directions pass the large cellular pool of potassium ions. The ratio of unidirectional $^{24}Na^+$ fluxes was time-variant and declined from an initial value of 3.66 ± 0.34 to a significantly smaller steady-state value of 2.57 ± 0.26 (P < 0.001, N = 5 paired observations), indicating that sodium ions pass the epithelium both via the paracellular and the cellular pathway. Quantitatively, the larger ratio of paracellular Na^+ fluxes, as compared to that of paracellular Cs^+ fluxes, is compatible with convective flow of the two alkali metal ions through the same population of water-filled pores. With a new set of equations, the fraction of the sodium flux passing the basement membrane barrier of the lateral space that is recirculated through the cellular compartment is estimated. This fraction was, on average, 0.72 ± 0.03 (N = 5). It is concluded that isotonicity of the transportate can be maintained by producing a hypertonic fluid emerging from the lateral space combined with reuptake of salt via the cells.

Key words: Small intestine — Leaky epithelia — Solute-coupled water transport — Na^+ recirculation — Lateral intercellular space — Flux ratio analysis

Introduction

Vertebrate small intestine, gallbladder, and renal proximal tubule belong to the class of leaky epithelia which has capacity for transporting isotonic fluid in the absence of transepithelial ion concentration-, electrical potential-, osmotic-, and hydrostatic-pressure differences. The transport of water depends on metabolic energy and on a simultaneous transport of NaCl with Na^+ submitted to active transport via Na^+/K^+-pumps. The transport of water can take place against an adverse osmotic gradient, but if the NaCl transport is abolished, water flow stops (Curran & Solomon, 1957; Windhager et al., 1958; Curran, 1959; Diamond, 1964*a*,*b;* Green et al., 1991). It is a major and unresolved problem to reconcile this metabolically energized rectified transport of water and NaCl in isotonic proportions under conditions of no external driving force with the major dissipative pathway for diffusible ions being localized between the epithelial cells.

In the classical category of models it is assumed that coupling between solute and water flows takes place in a macroscopic subcompartment (Curran & MacIntosh,

Correspondence to: S. Nedergaard

1962; Diamond & Bossert, 1967) supposed to build up osmotic and hydrostatic pressures above those of the bathing solutions. Generally, this compartment is assumed to be the lateral space between the epithelial cells. As yet, it has not been possible to assess the putative driving force for water movement into the space. And based on theoretical considerations it is likely that the tonicity of the fluid emerging downstream the space would be hypertonic, rather than truly isotonic (reviewed in Spring, 1998; Weinstein, 1988, 1992; Whittembury & Reuss, 1992). These difficulties have provided room for models assuming transport of water through the cells. As for example, via cloned water channels (Agre & Nielsen, 1996) in cell membranes with very high hydraulic water permeability (Schafer, 1990), or by way of solute coupled uphill water transport in membrane proteins associated with other functions, like a Na^+-glucose transporter, a Na^+-K^+-$2Cl^-$-transporter, and a Na^+-lactate transporter (Zeuthen, 1995).

With the Na^+-recirculation theory developed (Ussing & Eskesen, 1989) and further explored (Ussing, Lind & Larsen, 1996; Sørensen et al., 1998) in studies of the secretory frog skin gland, the type of models which assumes coupling of solute and water flow in the lateral intercellular space should be reevaluated. In this study is presented a method based on $^{134}Cs^+$ and $^{24}Na^+$ pre-steady state flux measurements for demonstrating paracellular convective flow of cations and for separating cellular and paracellular sodium fluxes in unperturbed toad small intestine. It is shown how these fluxes can be used for calculating the flux of sodium that is recirculated through the epithelial cells. Our experimental results will be used for discussing the significance of ion recirculation for producing an isotonic absorbate. The present investigation includes previous studies published in preliminary form (Ussing & Lind, 1996; Ussing & Nedergaard, 1993; Nedergaard & Ussing, 1997).

Materials and Methods

Animals and Experimental Preparation

Large female toads (*Bufo bufo*) caught in late summer were stored at 7°C in drawers in a pool of water. More than 10 days before the experiment the temperature of the bath was slowly raised (~24 hr) to 20°C. The toads were then transferred to a cage with hiding facilities, a water pool, and fed with *Tenebrio* larvae. After at least 10 days of eating *ad libitum*, the small intestine is well developed. The toad was decapitated and doubled pithed. A 2-cm long piece of small intestine cut from above one cm caudal to the pylorus valve was emptied by flushing with Ringer's solution and mounted as a tube in a glass chamber constructed for intestinal perfusion studies (Harvey & Nedergaard, 1964). The preparation was tied to the glass tube by soft cotton strings. The intestinal wall with an area of 1.57 cm^2 was exposed to 5 ml on the luminal side and 60 ml on the serosal side of identical Ringer's solution. Stirring was performed by aerating with oxygen. After an equilibration period of 30 min, the measurements were carried out under open-circuit conditions with an average transepithelial potential difference of, $V_t = -3.9 \pm 1.8$ mV ($N = 14$ preparations, serosal bath grounded).

Frogs (*Rana temporaria*) were kept in tap water at 4°C. The epithelium of double-pithed animals was isolated by serosal exposure of the skin to 2 mg/ml collagenase in Ringer's solution, and mounted in a flux chamber with 2 cm^2 exposed area supported by a steel mesh on the external surface. Following about 1 hr of equilibration at open circuit, the epithelium was short circuited and $^{134}Cs^+$ was added to the serosal bath. After 60 min the epithelium was washed for 30 min in non-radioactive Ringer's solution, and the radioactivity measured. For studying with the above protocol $^{134}Cs^+$ trapping at reduced sodium pump activity, prior to adding $^{134}Cs^+$ the serosal side the epithelium was exposed to ouabain at a submaximal concentration of 10^{-5} M.

Flux Measurements

As the transport properties change along the small intestine it is not possible to use two adjacent pieces of intestine for obtaining paired unidirectional fluxes. Flux-ratio analysis was therefore carried out by measuring the two unidirectional fluxes in one and the same preparation. During the initial period of about 40–70 min fluxes were measured in the direction from serosa to lumen. Then, following three times of gentle washings, fluxes from lumen to serosa were measured for a similar period of time. Every 5 min, samples of 1 ml were withdrawn from the chamber opposite to the one with the isotope added and replaced with 1 ml of fresh Ringer's solution. The volume activity of the hot chamber did not change during the period of flux measurements. With a sampling interval of 5 min, the flux per unit area of intestinal wall (total area: 1.57 cm^2) is given as the amount of tracer appearing on the *trans* side expressed in per cent (%) of the concentration of tracer (cpm · ml^{-1}) on the *cis* side:

$$M = \frac{100 \cdot (\Delta cpm \text{ in 5 min})_{trans\ side}}{1.57 \cdot (cpm \cdot ml^{-1})_{cis\ side}} [\% \cdot cm^{-2} \text{ in 5 min}].$$

Solutions, Radionucleides, and Chemicals

The Ringer's solution used in experiments with the intestinal preparation contained (mM): 117.4 Na^+, 2 K^+, 1 Ca^{2+}, 2 Mg^{2+}, 118 Cl^-, 2.4 HCO_3^-, 5 $acetate^-$, 5 glucose, pH = 8.2 when aerated with oxygen. In experiments with the isolated frog skin epithelium, the composition was, 113.4 Na^+, 1.9 K^+, 1 Ca^{2+}, 2 Mg^{2+}, 117.9 Cl^-, 2.4 HCO_3^-, pH = 8.2. $^{42}K^+$, $^{134}Cs^+$, and $^{24}Na^+$ were purchased from Risø, Roskilde (Denmark) with the following specific activities: ~42 GBq/g K as ^{42}KCl at a concentration of ~260 mBq/ml H_2O, ~800 GBq/g Cs as 'carrier free' $^{134}CsCl$ at a concentration of ~70 mBq/ml H_2O, and ~85 GBq/g Na as $^{24}NaCl$ at a concentration of ~265 mBq/ml H_2O. The radioactivity of the samples was counted in a Packard 1900TR Liquid Scintillation Analyzer using Ultima Gold scintillation cocktail (Packard). Trapped $^{134}Cs^+$ radioactivity was counted following disolution in Soluen-350 (Packard) of the preparation used for flux studies. Collagenase was from Boehringer-Mannheim (cat. no. 103586), and ouabain from Sigma (cat. no. O-3125).

Data Treatment

Results are given as mean ± SEM with N indicating the number of preparations entering the analysis. Means were compared by performing Student's *t*-test.

Results

In this study pathways taken by small diffusible cations are investigated by following the time course of tracer appearance in the solution opposite to the bath to which the isotope was added (time zero). Specifically, paracellular convective flows are studied by measuring pre-steady state fluxes of radiolabeled cesium ions (Ussing & Nedergaard, 1993; Ussing et al., 1996), and by analysing pre-steady-state fluxes of radio-labeled sodium ions. The pre-steady-state flux ratio theorem (Sten-Knudsen & Ussing, 1981) states that the ratio of unidirectional fluxes through a single pathway is time-invariant from the moment the tracers appear, and equal to the ratio of the unidirectional fluxes measured when the building up of the tracers along the pathway are at steady state. A corollary to this theorem is that if, at physiological steady state, the flux ratio is time variant the ion in question makes use of two or more pathways with different flux ratios and mean passage times. Rather than hydrophilic nonelectrolytes, cesium is used for tracing paracellular solvent drag. Experimental evidence will be discussed that this monovalent cation tracer passes the epithelium via an extracellular route which is also shared by sodium ions.

The Use of Radio-Labelled Cs^+ for Tracing Paracellular Fluxes

The rationale of the Cs^+ method can be illustrated by experiments with the frog skin. If almost carrier-free $^{134}Cs^+$ is added to the isolated frog skin epithelium the isotope is trapped in proportion to the active flux of Na^+ (Fig. 1). It can be seen that the relationship between the amount of $^{134}Cs^+$ trapped by the epithelial cells and the activity of the Na^+/K^+-pump measured as the short-circuit current depicts a straight line, which passes through the origin. This simple relationship holds over a wide range of Na^+ fluxes whether the variation of the active flux is due to the spontaneous activity of different preparations, or to a partial inhibition of the sodium pump by ouabain added to the solution bathing the serosal side of the isolated epithelium. Thus, radioactive Cs^+ enters the cells via the Na^+/K^+-pump (competing with K^+), and independent of the turnover of the cellular Na^+ and K^+ pools, once $^{134}Cs^+$ has entered the cells it is virtually irreversibly trapped in this compartment. A corollary to this observation is that if $^{134}Cs^+$ is recovered from the solution opposite to the solution to which the tracer is added it must have passed the epithelium exclusively via the paracellular pathway.

Comparison of Fluxes of $^{42}K^+$ and $^{134}Cs^+$ Across Toad Small Intestine

In Fig. 2 is shown that it takes the two tracers, $^{134}Cs^+$ and $^{42}K^+$, different times for reaching a steady flux. The appearance of $^{134}Cs^+$ both in the luminal perfusion solution (Fig. 2, *left hand panel*) and in the serosal bath (Fig. 2, *right hand panel*) is relatively fast. In contrast, the appearance of $^{42}K^+$ was so slow that a steady state was not reached within the observation period of 70 min. The fact that the K^+ fluxes at all times are significantly smaller than the simultaneously measured Cs^+ fluxes also indicates that the potassium flux has not reached steady state toward the end of the observation period. The examples shown here are representative of a total of 9 experiments and in none of the experiments was it possible to derive a half time or any other quantitative measure of the time course of appearance of $^{42}K^+$ on the *trans* side of the preparation. This finding indicates that, whether the tracer is added to the luminal or the serosal bath, a significant component of $^{42}K^+$ passes the large cellular pool of long turnover time constant. The cesium tracer, on the other hand, passes the intestinal epithelium via a much faster route, i.e., this ion seems to move through the intestinal epithelium between the cells.

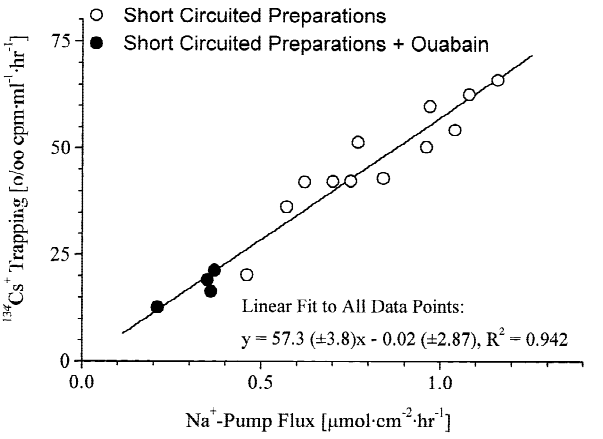

Fig. 1. Dependence of intracellular trapping of $^{134}Cs^+$ on active transport of Na^+ in frog skin epithelium. [Ouabain] on serosal side was 10 μM. The amount of radioisotope trapped is expressed as ‰ of cpm in 1 ml of inside bath per hour per cm^2 of isolated epithelium. The active flux was calculated from the continuously monitored short-circuit current. The line of regression indicates that the y-intercept is not significantly different from zero.

Fluxes of $^{134}Cs^+$ in the Intestinal Preparation

In the following experiments the lumen-to-serosa flux and the serosa-to-lumen flux were obtained from the same preparation as explained in the method section. In the example shown in Fig. 3 (*left hand panel*), the rate constant of the time course of tracer appearance was, 0.115 min^{-1} for the influx and 0.127 min^{-1} for the efflux, corresponding to half times, $T_{1/2}$ = 6.0 and 5.5 min, respectively. The flux ratio was constant from the time of appearance of tracers (Fig. 3, *right hand panel*) in

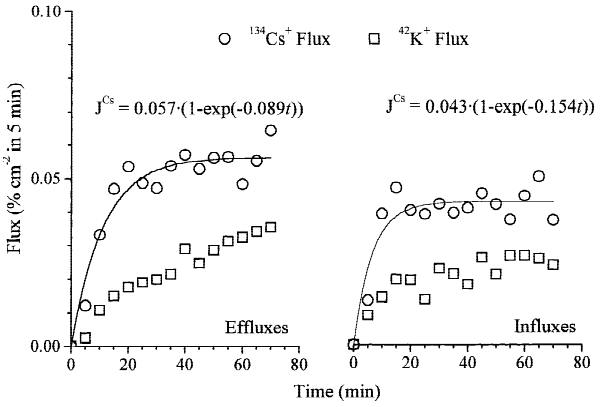

Fig. 2. Unidirectional fluxes of $^{42}K^+$ and $^{134}Cs^+$ in toad small intestine. *Left hand panel:* The effluxes of the two isotopes were measured in the same piece of preparation. *Right hand panel:* The influxes were also measured in the same piece of intestinal preparation, but from another animal than the one used for the efflux measurements. The time course of the $^{134}Cs^+$ appearance was fitted with a monoexponential time function providing estimates of the half time of tracer equilibration and the steady-state unidirectional flux. The fluxes of ^{42}K did not reach steady state within the observations period of 70 min and could not be evaluated quantitatively.

agreement with the notion forwarded above that just a single route, the paracellular pathway, is available for transepithelial transport of radiolabeled cesium ions. For this preparation, the steady state flux-ratio was, $(M^{\infty}_{ms}/M^{\infty}_{sm})_{Cs} = (0.136/0.068) = 2.00$. Results of a total of 6 paired experiments are collected in Table 1. The half time of tracer appearance differed among the preparations by a factor of two, but was about the same in the two directions when fluxes measured in the same preparation are compared.

In all preparations was the lumen-to-serosa flux larger than the serosa-to-lumen flux. This asymmetry of unidirectional fluxes shows that an inwardly directed driving force is imposed on radio-labeled cesium ions. The force, E, is given by (Ussing, 1952):

$$E = \frac{R \cdot T}{F} ln \left(\frac{M^{\infty}_{ms}}{M^{\infty}_{sm}} \right)_{Cs} \qquad (1a)$$

And for the case of paracellular transport of $^{134}Cs^+$ with the steady state flux being the result of both an electrodiffusion and a convection process, the flux-ratio equation takes the form:

$$R \cdot T \cdot ln \left(\frac{M^{\infty}_{ms}}{M^{\infty}_{sm}} \right)_{Cs} = R \cdot T \cdot ln \frac{a^{m}_{Cs}}{a^{s}_{Cs}} + F \cdot V_t + \frac{R \cdot T \cdot J_V}{D_{Cs}} \cdot \int_{x=0}^{x=\delta} \frac{1}{A(x)} dx \qquad (1b)$$

Where a^{m}_{Cs} and a^{s}_{Cs} are the activities of Cs^+ in mucosal (^{m}) and serosal (^{s}) bath, V_t the transepithelial potential difference, D_{Cs} the diffusion coefficient for Cs^+ in water, J_V the water flux (positive in inward direction), and $A(x)$ the cross sectional area of the paracellular route of length δ, which varies in an unknown manner with distance, x. With similar $^{134}Cs^+$ activity in the bathing solutions and $V_t = -3.9 \pm 1.8$ mV, the ratio of unidirectional electrodiffusion fluxes would be less than unity and, $E = -3.9$ mV (i.e., outwardly directed, Eq. 1*b*). The flux ratio of 2.06 ± 0.12 (Table 1) corresponds to an average inwardly directed driving force of $E = 18.2 \pm 1.5$ mV (Eq. 1*a*). This observation leads to the conclusion that the flux of $^{134}Cs^+$ is governed by a large solvent drag component (Eq. 1*b*). It was also found, that in toad small intestine the amount of $^{134}Cs^+$ trapped by the cells (i.e., entering the cells via the Na^+/K^+-pump) is linearly correlated with the lumen-to-serosa flux of $^{134}Cs^+$ (Fig. 4), indicating that the Na^+/K^+-pumps are located on the membranes facing the lateral intercellular space (*see* Discussion). The above results (Figs. 2–4, Table 1) lead to the following notions about $^{134}Cs^+$ fluxes in toad small intestine, (i) just a single transepithelial pathway is available for $^{134}Cs^+$, (ii) this pathway is paracellular, and (iii) the net inward paracellular flux of $^{134}Cs^+$ is brought about by solvent drag.

Fluxes of $^{24}Na^+$ in the Intestinal Preparation

Figure 5 shows an example of $^{24}Na^+$ flux measurements performed with a protocol similar to the one discussed above. Generally, steady state fluxes could be determined with an observation period of 40–50 min. In contrast to results obtained with $^{134}Cs^+$, the ratio of unidirectional $^{24}Na^+$ fluxes was not constant in time. As shown in Fig. 5 (*right hand panel*), the flux-ratio was large to begin with and declined toward a stationary value achieved in the course of the subsequent sampling periods. Thus, more than one pathway is available for transport of sodium ions through the intestinal epithelium. These pathways have different flux ratios and different passage times. This result, which is similar to that obtained for frog skin (Ussing et al., 1981), shows that $^{24}Na^+$ besides the fast paracellular shunt also passes the slow cellular route. It can also be seen (Fig. 5, *right hand panel*) that the $^{24}Na^+$ flux-ratio of the faster paracellular route is larger than that of the slow cellular route. Assuming that only (these) two pathways are available for transepithelial sodium transport a set of four equations can be constructed from which the steady-state unidirectional fluxes through the two pathways can be estimated. Considering appearing fluxes, the time-dependent unidirectional fluxes in the inward and the outward direction, $M_{ms}(t)$ and $M_{sm}(t)$, can be written:

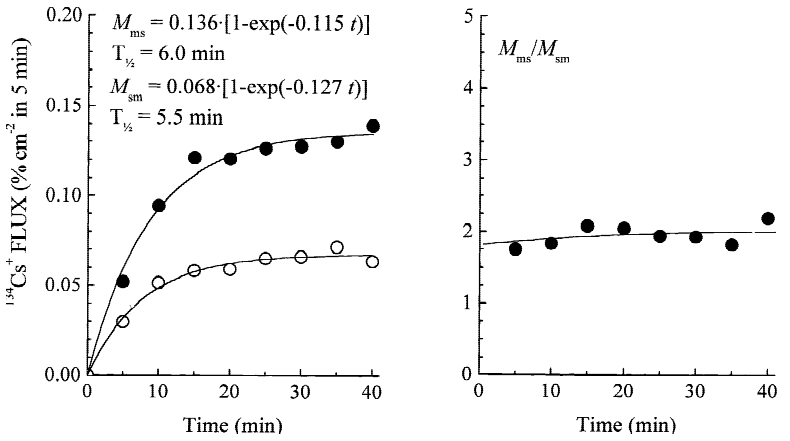

Fig. 3. Unidirectional fluxes of $^{134}Cs^+$ measured in the same piece of isolated small intestine of the toad. *Left hand panel:* When studying the fluxes in the two directions in the same piece of epithelium, similar half times of tracer appearance was observed. The steady-state influx of $^{134}Cs^+$ was significantly larger than the steady-state efflux. Symbols: ● is the flux from mucosa to serosa (M_{ms}); o is the flux from serosa to mucosa (M_{sm}). *Right hand panel:* The flux ratio was constant in time indicating that just a single pathway is available for transport of $^{134}Cs^+$ across the intestinal epithelium. The line indicates the ratio calculated from the fitted curves of the left hand panel.

Table 1. Radio-labeled cesium fluxes across toad small intestine

Prep. #	$T_{½}$ (ms)	$T_{½}$ (sm) min	M^{∞}_{ms}	M^{∞}_{sm} % cm^{-2} in 5 min	$M^{\infty}_{ms}/M^{\infty}_{sm}$
A1	4.3	5.8	0.177	0.085	2.09
A2	6.0	5.5	0.136	0.068	2.00
A3	6.1	6.2	0.143	0.078	1.83
A4	9.4	9.1	0.260	0.100	2.60
A5	4.3	5.0	0.127	0.060	2.13
A6	4.6	5.9	0.184	0.106	1.73
				Mean ± SEM	2.06 ± 0.12

Unidirectional fluxes in the mucosa-to-serosa (ms) and serosa-to-mucosa (sm) direction were measured in the same preparation. Results of experiments with 6 preparations are shown. The time dependence of the fluxes was fitted with a monoexponential time function for estimating the half time of tracer appearance, $T_{½}$, and the steady-state unidirectional fluxes, M^{∞}_{ms} and M^{∞}_{sm}, conf. Fig. 2.

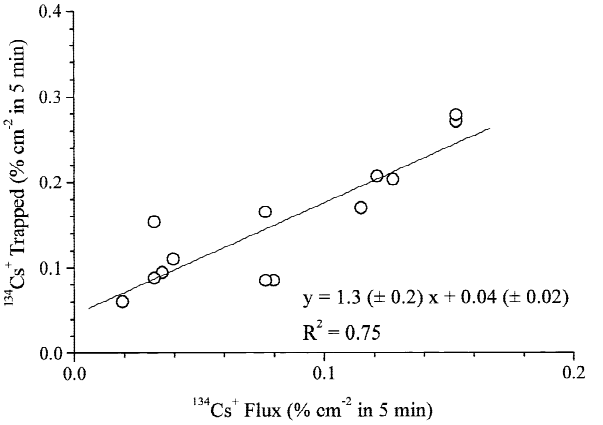

Fig. 4. Trapping of $^{134}Cs^+$ in the intestinal epithelium of toad as a function of the convective flow of $^{134}Cs^+$ in the direction from lumen to serosa.

$$M_{ms}(t) = J^{para}_{ms} \cdot [1 - g(t)] + J^{active}_{ms} \cdot [1 - f(t)] \quad (2a)$$

$$M_{sm}(t) = J^{para}_{sm} \cdot [1 - g(t)] + J^{active}_{sm} \cdot [1 - f(t)] \quad (2b)$$

Here $g(t)$ and $f(t)$ are functions of time with the following initial and boundary conditions, $g(t) = f(t) = 1$ for $t = 0$, and $g(t) = f(t) = 0$ for $t \to \infty$. J^{para}_{ms} and J^{para}_{sm} are the steady-state unidirectional paracellular fluxes, and J^{active}_{ms} and J^{active}_{sm} are the steady-state unidirectional cellular fluxes. The reason also for denoting the serosa-to-lumen transcellular flux "active" will be made obvious in Discussion. If $g(t)$ approaches zero much faster than $f(t)$, there is a time interval, $0 < t < t_1$, for which a set of values, $[\tau_1, M(\tau_1)]$, obeys the relationships:

$$M_{ms}(\tau_1) = J^{para}_{ms} \cdot [1 - g(\tau_1)] \quad (3a)$$

$$M_{sm}(\tau_1) = J^{para}_{sm} \cdot [1 - g(\tau_1)] \quad (3b)$$

where $\tau_1 < t_1$. Similarly, there is a time interval, $t_2 < t < \infty$, for which at a set of values, $[\tau_2, M(\tau_2)]$, obeys the relationships:

$$M_{ms}(\tau_2) = J^{para}_{ms} + J^{active}_{ms} \cdot [1 - f(\tau_2)] \quad (4a)$$

$$M_{sm}(\tau_2) = J^{para}_{sm} + J^{active}_{sm} \cdot [1 - f(\tau_2)] \quad (4b)$$

where $\tau_2 > t_2$. Thus, we can write:

$$\frac{M_{ms}(\tau_1)}{M_{sm}(\tau_1)} = \frac{J^{para}_{ms}}{J^{para}_{sm}}, \text{ for } \tau_1 < t_1 \quad (5a)$$

$$\frac{M_{ms}(\tau_2) - J^{para}_{ms}}{M_{sm}(\tau_2) - J^{para}_{sm}} = \frac{J^{active}_{ms}}{J^{active}_{sm}}, \text{ for } \tau_2 > t_2 \quad (5b)$$

It follows from definitions:

$$M^{\infty}_{ms} = J^{para}_{ms} + J^{active}_{ms} \quad (5c)$$

$$M^{\infty}_{sm} = J^{para}_{sm} + J^{active}_{sm} \quad (5d)$$

Taking the experiment shown in Fig. 5 as an example, the calculations are based on the following asymptotic

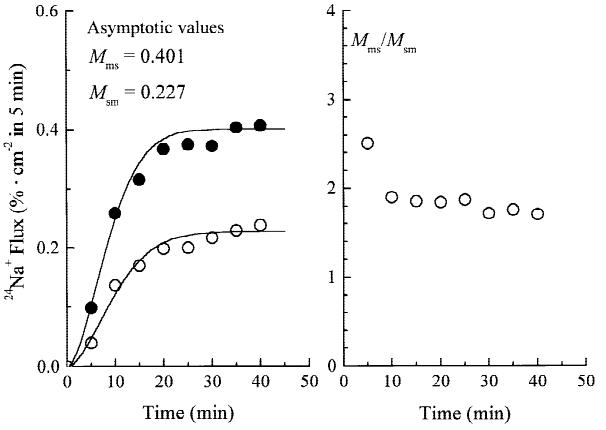

Fig. 5. Unidirectional tracer fluxes of $^{24}Na^+$ across the same piece of toad small intestine. *Left hand panel.* Symbols: ● is the flux from mucosa to serosa (M_{ms}); o is the flux from serosa to mucosa (M_{sm}). Similar to the $^{134}Cs^+$ fluxes, was the steady-state flux ratio for Na^+, $M^{\infty}_{ms}/M^{\infty}_{sm} > 1$. *Right hand panel:* The flux ratio was not constant in time indicating that more than one pathway is available for transepithelial sodium movement.

values, $M^{\infty}_{ms} = 0.401$ and $M^{\infty}_{sm} = 0.227$. By choosing $\tau_1 = 5$ min with $M_{ms}(5) = 0.099$ and $M_{sm}(5) = 0.039$, and $\tau_2 = 15$ min with $M_{ms}(15) = 0.315$ and $M_{sm}(15) = 0.170$, we obtain (Eqs. 5), $J^{para}_{ms} = 0.145$, $J^{para}_{sm} = 0.056$, $J^{active}_{ms} = 0.256$, and $J^{active}_{sm} = 0.171$, respectively, with all fluxes in % · cm^{-2} in 5 min.

We shall now be dealing with steady state fluxes, only, and will use, therefore, the conventional unit of pmol · cm^{-2} · sec^{-1}. With a concentration of Na^+ in the bathing solutions of 117.4 μmol · cm^{-3} the conversion factor is, $117.4 \cdot 10^6/(5 \cdot 60 \cdot 100) = 3.91 \cdot 10^3$. In Table 2 are listed steady-state unidirectional fluxes through the two pathways for five preparations obtained by the method presented above. According to these estimates both the cellular and the paracellular pathway carry a significant net flux in the inward direction. The paracellular driving force is (Eq. 1*a*), $E = 32.3 \pm 2.5$ mV, which indicates transport of sodium between the cells by a convection process. Thus, the drag force imposed on the sodium ions is larger than that calculated from the cesium experiments, i.e., 32.3 ± 2.5 mV for Na^+ *vs.* 18.2 ± 1.5 mV for Cs^+. If the two ions move through the same population of water-filled pores, we would expect that the drag on the sodium ions is larger than the drag on the cesium ions (stemming from the fact that the ratio of the diffusion coefficients, $D_{Cs}/D_{Na} = 1.5$, e.g., Eq. 1*b*). For the limiting case of no discrimination along the route between the two alkali ions, we can assume for the convection process, $(J^{para}_{ms}/J^{para}_{sm})_{Na} = (J^{para}_{ms}/J^{para}_{sm})^{D_{Cs}/D_{Na}}_{Cs}$. Accordingly, the predicted ratio of unidirectional paracellular Na^+ fluxes would be, $(J^{para}_{ms}/J^{para}_{sm})^{D_{Cs}/D_{Na}}_{Cs} \approx 2.06^{1.5} = 2.96$ (Table 1), which is not identical with, but fairly close to the measured paracellular sodium-flux ratio of 3.66 ± 0.34 listed in Table 2.

Discussion

Pathways and Cell Membrane Transporters in Vertebrate Small Intestine

This study presents evidence that in toad small intestine $^{134}Cs^+$ is transported by convection along the paracellular pathway (Fig. 3, Table 1). It was found that the amount of $^{134}Cs^+$ trapped by the cells while passing the paracellular pathway is linearly correlated to the flux of $^{134}Cs^+$ directed from lumen to serosa (Fig. 4). The experiments with frog skin (Fig. 1) showed that $^{134}Cs^+$ enters the epithelial cells via Na^+/K^+-pumps. Taken together, the results indicate that in toad small intestine the Na^+/K^+-pumps are located along the paracellular route, i.e., on the membranes facing the lateral intercellular space. Interestingly, the flux of $^{134}Cs^+$ pumped into the cells is of a magnitude similar to that passing the paracellular route, i.e., every second $^{134}Cs^+$ ion flowing into the lateral space is pumped into the cells rather than proceeding via the low resistance pathway into the serobal bath. Since this result is independent of the convection flux of $^{134}Cs^+$, it is indicated that the convection process is driven by the Na^+/K^+-pumps. The study also presents estimates of unidirectional steady-state fluxes of $^{24}Na^+$ through paracellular and cellular pathways in unperturbed intestinal preparations. It is a major finding that both pathways carry significant net fluxes in inward direction (Fig. 5, Table 2). Like the flux of $^{134}Cs^+$, also the paracellular flux of $^{24}Na^+$ is governed by a convection process.

The model of the epithelium of vertebrate small intestine shown in Fig. 6 contains paracellular and transcellular pathways for ion movements. It depicts the paracellular pathway as the route of transepithelial water flow under isotonic conditions, and contains membrane transporters that translocate the major ions, Na^+, Cl^-, and K^+ across the cell. A common cell type expresses both absorptive and secretory functions. First, we briefly discuss studies leading to this model. Next, we derive equations for estimating recirculation fluxes of Na^+ contained in the model (arrows). Finally, we discuss the physiological significance of ion recirculation driven by the lateral Na^+/K^+-pump for the generation of an isotonic transportate.

The Paracellular Route

According to studies of the voltage dependence of transepithelial unidirectional fluxes in rabbit ileum about 85% (~8 mS · cm^{-2}) of the transepithelial electrical conduc-

Table 2. Unidirectional steady state Na^+ fluxes (pmol · sec^{-1} · cm^{-2})* across glucose-stimulated toad small intestine exposed to isotonic Ringer on the mucosal and the serosal side

Prep. #	M_{ms}^{∞}	M_{sm}^{∞}	$\frac{M_{ms}^{\infty}}{M_{sm}^{\infty}}$	J_{sm}^{para}	J_{sm}^{para}	$\frac{J_{ms}^{para}}{J_{sm}^{para}}$	J_{ms}^{active}	J_{sm}^{active}
B1	1070	370	2.90	400	100	4.00	670	270
B2	1570	890	1.76	570	220	2.59	1000	670
B3	1070	405	2.64	500	125	4.00	570	270
B4	1620	720	2.25	320	100	3.20	1300	620
B5	1320	400	3.30	450	100	4.50	870	300
Mean	1330	560	2.57	450	130	3.66	880	430
±SEM	±120	±100	0.26	±40	±20	±0.34	±130	±90

* The steady state unidirectional fluxes were estimated from Eqs. 5 as explained in the text.

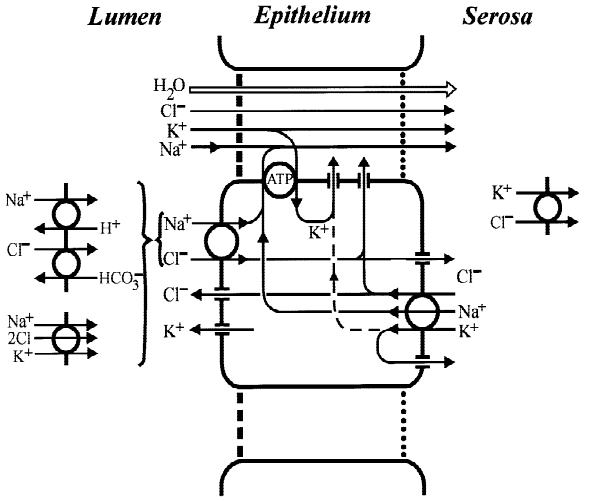

Fig. 6. Ion pathways and recirculating fluxes associated with transepithelial (paracellular) fluid transport in vertebrate small intestine. Water flows between the cells. Ion fluxes contain both paracellular convective- and cellular active components. *Inset left:* Electroneutral uptake of NaCl mediated by a set of double exchangers or by cotransport with K^+. *Inset right:* Electroneutral coupled exit of KCl in inner membrane. Sodium is also taken up with glucose and amino acids (*not shown*).

tance is associated with ion flows between the cells (Frizzell & Schultz, 1972). A microelectrode study of the conductance of the individual membranes confirmed that the paracellular conductance of (flounder) small intestine accounts for a significant fraction (~95%) of the transepithelial conductance (~27 mS · cm^{-2}, Halm, Krasney & Frizzell, 1985*a*). Pappenheimer and coworkers provided evidence that not only small electrolytes but also dietary monosaccharides and amino acids can be transported between the cells (reviewed in Pappenheimer, 1993). The existence of paracellular water transport is further supported by the finding that the lateral intercellular space of ileal mucosa was dramatically expanded in response to glucose-activated fluid transport (Atisook et al., 1990). The general conclusion from these studies is that a paracellular flow of water drags molecules, which can penetrate the junction membrane in the inward direction. This is compatible with our experiments with $^{134}Cs^+$ (Figs. 2 and 3, Table 1) and $^{24}Na^+$ (Fig. 5, Table 2) indicating that fluxes of these ions contain significant convection components flowing through a common population of junctional pores. It is also in agreement with observed convection flows of ions and small hydrophilic molecules in other leaky vertebrate epithelia, e.g., gallbladder (Hill & Hill, 1978; Whittembury et al., 1980) and kidney proximal tubule (Frömter, Rumrich & Ullrich, 1973; Whittembury et al., 1988).

Cellular Pathways

Unlike a number of other fluid absorbing epithelia water channels have not been found in epithelial cells of small intestine (Nielsen et al., 1993). There is unanimous agreement that Na^+/K^+-pumps are localized to the lateral membranes (Fig. 6). As discussed above, our studies led to this conclusion, and following studies by Schultz & Zalusky (1964) indicating active Na^+ transport energized by ouabain inhibitable Na^+/K^+-pumps, Stirling (1972) showed that radio-labeled ouabain binds specifically to the membranes facing the lateral intercellular space. In agreement with early studies (reviewed in Frizzel, Field & Schultz, 1979) the apical uptake of Na^+ is depicted as an electroneutral process coupled to entry of Cl^- against this ion's electrochemical gradient (Fig. 6). The apical NaCl uptake may not result from obligatory one-for-one cotransport via a common apical transport protein but, rather, involves a set of parallel Na^+/H^+ and Cl^-/HCO_3^- exchangers (Turnberg et al., 1970) of which the gene coding for the Na^+/H^+ exchanger (NHE-3) has been cloned (Tse, Brant & Walker, 1992). This set of transporters are indicated in the *left hand inset* of Fig. 6, which also contains, in agreement with studies of flounder (Halm et al., 1985*b*), a Na^+-K^+-$2Cl^-$ cotransporter together with a K^+-selective channel. Also glucose and amino acids are transported across the epithelial cells by mechanisms which involve Na^+ gradient-driven uptake

across the luminal membrane (Schultz & Curran, 1970), of which the gene (SGLT1) coding for the apical Na-glucose transporter has been cloned (Hediger et al., 1987). The apical Cl^- channel mediates the cAMP-stimulated secretion energized by the Na^+/K^+-pump via furosemide inhibitable (Na^+-K^+-$2Cl^-$)-cotransport across the inner membrane (Frizzell et al., 1979). In cell attached patch-clamp studies of *Necturus* enterocytes, Giraldez et al. (1989) identified an outward rectifying secretory Cl^- channel with a conductance of 17–25 pS (depending on membrane voltage) activated by raising cellular [cAMP], but not by cytosolic Ca^{2+} or membrane depolarization. Since cellular Cl^- and K^+ both are above electrochemical equilibrium, Frizzell et al. (1979) assumed that these ions move by electrodiffusion (in selective channels, Fig. 6) from cell to serosal bath. More recent studies of flounder intestinal mucosa have indicated transport of Cl^- and K^+ also by way of electroneutral exit via a common mechanism (Halm et al., 1985*b*), perhaps similar to the K^+-Cl^- cotransporter first identified by Reuss (1983) in gallbladder epithelial cells. In agreement with their hypothesis this transporter is added in the *right hand inset* of Fig. 6.

The model of Fig. 6 depicts Cl^- absorption and Cl^- secretion as being confined to one and the same cell type. In the literature it has been discussed that in mammalian small intestine these two fluxes of opposite direction are located in different cells (Madara, 1991; Sullivan & Field, 1991). However, an intracellular microelectrode study of *Necturus* small intestine (Giraldez & Sepulveda, 1987) showed that stimulation of alanine uptake resulted in membrane depolarization in cells of which an apical Cl^- conductance was stimulated simultaneously. This observation indicates that absorption and secretion in this species are co-expressed. In the recirculation theory discussed below it is not of importance whether Cl^- returns via the absorbing cell or another cell type. As studies of non-mammalian intestinal epithelium did not indicate cellular heterogeneity, we consider it appropriate, at this stage of the analysis, to place the chloride channels of the model of amphibian small intestine in the absorbing cell, noting that this localization is not yet settled with certainty.

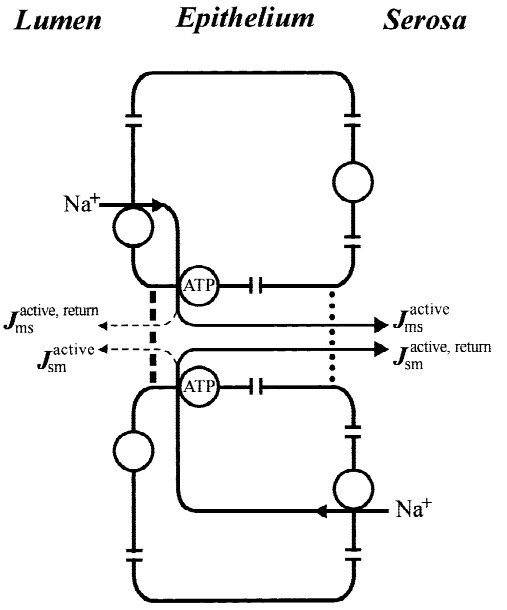

Fig. 7. Diagram designed for assisting the analysis of the forward and backward cellular pathways of unidirectional $^{24}Na^+$ fluxes. *Upper part:* Influx path. *Lower part.* Outflux path. J_{ms}^{active} and J_{sm}^{active} are the forward and backward active fluxes, respectively. The 'return' fluxes ($J_{ms}^{active,\ return}$ and $J_{sm}^{active,\ return}$) are 'invisible' components related to the two other components as indicated by Eqs. (6) in text. The relatively smaller components moving into the luminal bath through the junction membrane are depicted with dashed arrows.

Estimation of the Sodium Recirculation Flux

The results of Table 2 indicate fairly large cellular Na^+ fluxes in both directions across toad small intestine. According to the model of the intestinal epithelium (Fig. 6), both of these fluxes pass the lateral Na^+/K^+-pumps, and are therefore active. In Fig. 7 we have depicted the pathways supposed to be taken by a sodium tracer passing the lateral Na^+/K^+-pump when added to the luminal fluid (*upper cell* of Fig. 7) or to the serosal bath (*lower cell* of Fig. 7), respectively. The inwardly (lumen-to-serosa) directed active Na^+-flux (J_{ms}^{active}) passes the apical membrane together with Cl^- and/or glucose, and is pumped into the lateral intercellular space from which it proceeds to the serosal bath. A fraction of the tracer flux entering the lateral space returns to the luminal solution via the Na^+ permeable junction membrane. This "invisible" component is denoted, $J_{ms}^{active,\ return}$. In the lower part of Fig. 7 is depicted the tracer flux in the opposite direction, J_{sm}^{active}, which passes the Na^+-K^+-$2Cl^-$ cotransporter in the basal membrane and is pumped into the lateral space from which it continues into the luminal solution via the junction membrane. The "invisible" component that passes downstream the lateral space for returning to the serosal bath is denoted, $J_{sm}^{active,\ return}$. We can now write:

$$\frac{J_{ms}^{active}}{J_{ms}^{active,\ return}} = \frac{J_{ms}^{para}}{J_{sm}^{para}} \tag{6a}$$

$$\frac{J_{sm}^{active,\ return}}{J_{sm}^{active}} = \frac{J_{ms}^{para}}{J_{sm}^{para}} \tag{6b}$$

which follows from the principle that a source delivering a substance at constant rate into a reversible pathway does not influence the ratio of unidirectional fluxes appearing from the two ends of the pathway (Ussing, 1952). With the cellular and paracellular fluxes taken

Table 3. Recirculation of Na^+ in toad small intestine

Prep.	$J_{sm}^{active,\ return}$	$J_{ms}^{active,\ return}$	$\frac{M_{ms}^{\infty} - M_{sm}^{\infty}}{(J_{ms}^{active} + J_{sm}^{active,\ return}) + (J_{ms}^{para} - J_{sm}^{para})}$
B1	1080	170	0.34
B2	1740	380	0.22
B3	1080	140	0.33
B4	1980	400	0.26
B5	2790	190	0.23
Mean	1730	260	0.28
±SEM	±320	±60	±0.03

Here are listed the "invisible" return fluxes (*see* Fig. 7), and the fraction of the paracellular Na^+ flux through the basement membrane barrier which is being added to the serosal compartment (column 4). With Eqs. (6*a*,*b*) in the text, the calculations were based on the fluxes presented in Table 2. Fluxes listed in column 2 and 3 are in pmol · sec^{-1} · cm^{-2}.

from Table 2, Eqs. (6*a*,*b*) were used to calculate the two "invisible" (return) flux components collected in Table 3. At steady state, the net flux crossing the basement membrane barrier is, $\sum J^{BM} = J_{ms}^{active} + J_{sm}^{active,\ return} + J_{ms}^{para} - J_{sm}^{para}$, while the flux added to the serosal bath is, $\Delta M^{\infty} = M_{ms}^{\infty} - M_{sm}^{\infty}$, and the flux returning from the serosal bath via the cotransporter is, $J_{sm}^{active} + J_{sm}^{active,\ return}$. Accordingly, the flux added to the serosal bath expressed as fraction of the total net inward flux is given by:

$$\frac{\Delta M^{\infty}}{\sum J^{BM}} = \frac{M_{ms}^{\infty} - M_{sm}^{\infty}}{(J_{ms}^{active} + J_{sm}^{active,\ return}) + (J_{ms}^{para} - J_{sm}^{para})} \qquad (7)$$

This fraction is listed in the fourth column of Table 3. According to these calculations, with similar Ringer's on the two sides of the intestinal epithelium the flux of sodium added to the serosal side constitutes only 28% of the net flux appearing downstream the lateral space. On average 72% returns by active transport to the lateral space. This latter component represents the Na^+ recirculation-flux.

Ion Recirculation in Toad Small Intestinal Epithelium

In the model of the absorbing intestinal epithelium shown in Fig. 6, the lateral space is separated from the luminal solution by the junction membrane. Another barrier is depicted at the level of the basement membrane and it separates the lateral space from the serosal bath. With water flowing in the inward direction both barriers have to be water permeable with the reflection coefficient of the junction membrane being larger than that of the basement membrane barrier, i.e., $\sigma^{JM} > \sigma^{BM}$. With Na^+/K^+-pumps in the plasma membranes facing the lateral intercellular space, Na^+ is pumped from the cells into the lateral space. Energized by the sodium gradient the cellular $[Cl^-]$ is maintained above thermodynamic equilibrium. Thus, this ion may be accumulated in the lateral space at a concentration above that of the bathing solutions by electrodiffusion from the cells through channels in the membranes lining the lateral space. As a result, energized by Na^+/K^+-pumps a hypertonic and hyperbaric lateral intercellular solution is generated providing the condition for water flow from lumen to the lateral intercellular space through the apical junction membrane. The fluid is flowing into the serosal compartment driven by a hydrostatic pressure difference between the lateral and the serosal compartments. By maintaining, simultaneously, a relatively large back flux of Na^+ (and Cl^-) from the serosal bath into the epithelial cells (Table 3), the epithelium has the capacity of creating an absorbate which is isotonic with the bathing solutions. According to the model in Fig. 6, the recirculation of Na^+ and Cl^- is due to cotransport with K^+ across the plasma membrane facing the serosal compartment. While Na^+ is pumped into the lateral space, a fraction of the Cl^- entering the cell via the basal cotransporter proceeds to the lateral space and the mucosal bath, respectively, while—supposedly—a smaller fraction, together with some K^+, returns directly to the serosal bath. Potassium selective channels in the lateral plasma membranes are supposed to return K^+ to the lateral space at a rate sufficiently large for maintaining a time-invariant $[K^+]$ of the lateral intercellular fluid. Thus, at steady state, the transport of K^+ into this space, by solvent drag through the junction membrane and by electrodiffusion through lateral channels, respectively, is equal to the sum of the active K^+ reuptake via the lateral Na^+/K^+ pumps and the K^+ flux escaping downstream to the serosal bath.

Physiological Significance of Sodium Recirculation

The sodium ions pumped from the cells into the lateral intercellular fluid are derived both from the mucosal and the serosal bath, with the latter component being the recirculating flux. By regulation of the flux recirculating through the cells a balance can be maintained between the paracellular forward and cellular backward flux of sodium such that the net transport of salt and the paracellular flow of water occur in isotonic proportions. In previous models considering coupling of solute and water flows in an intraepithelial compartment (Curran & MacIntoch, 1962; Diamond & Bossert, 1968) metabolic energy is invested only in the generation of a hypertonic and hyperbaric solution within the epithelium (the paracellular space). The subsequent formation of an isotonic transportate was postulated to be a purely dissipative process. According to the sodium recirculation theory, metabolic energy is not only spent in driving water into

the epithelium, but also in making the transportate isotonic.

Thanks are due to Mrs. Fritze Lind for skilled laboratory assistance in performing the experiments shown in Fig. 1. The study was supported by grants from the Alfred Benzon, Carlsberg, and Novo-Nordisk Foundations, and the Danish Natural Science Research Council (grant 11-0971).

References

Agre, P., Nielsen, S. 1996. The aquaporin family of water channels in kidney. *Nephrologie* **17:**409–415

Atisook, K., Carlson, S., Madara, J.L. 1990. Effects of phlorizin and sodium on glucose-elicited alterations of cell junctions in intestinal epithelia. *Am. J. Physiol.* **258:**C77–C85

Curran, P.F. 1959. Na, Cl, and water transport by rat ileum in vitro. *J. Gen. Physiol.* **43:**1137–1148

Curran, P., MacIntosh, J.R. 1962. A model system for biological water transport. *Nature* **193:**347–348

Curran, P.F., Solomon, A.K. 1957. Ion and water fluxes in the ileum of rats. *J. Gen. Physiol.* **41:**143–168

Diamond, J.M. 1964*a*. Transport of salt and water in rabbit and guinea pig gall bladder. *J. Gen. Physiol.* **48:**1–14

Diamond, J.M. 1964*b*. The mechanism of isotonic water transport. *J. Gen. Physiol.* **48:**15–42

Diamond, J.M., Bossert, W.H. 1967. Standing gradient osmotic flow. A mechanism for coupling of water and solute transport in epithelia. *J. Gen. Physiol.* **50:**2061–2083

Frizzell, R.A., Field, M., Schultz, S.G. 1979. Sodium-coupled chloride transport by epithelial tissues. *Am. J. Physiol.* **236:**F1–F8

Frizzell, R.A., Schultz, S.G. 1972. Ionic conductances of extracellular shunt pathway in rabbit ileum. Influence of shunt on transmural sodium transport and electrical potential. *J. Gen. Physiol.* **59:**318–346

Frizzell, R.A., Smith, P.L., Vosburgh, E., Field, M. 1979. Coupled sodium-chloride influx across brush border of flounder intestine. *J. Membrane Biol.* **46:**27–39

Frömter, E., Rumrich, G., Ullrich, K.J. 1973. Phenomenological description of Na^+, Cl^- and HCO_3^- absorption. *Pfluegers Arch.* **343:**189–220

Giraldez, F., Murray, K.J., Sepulveda, F.V., Sheppard, D.N. 1989. Characterization of a phosphorylation-activated Cl^- selective channel in isolated *Necturus* enterocytes. *J. Physiol.* **416:**517–537

Giraldez, F., Sepulveda, F.V. 1987. Changes in the apparent chloride permeability of *Necturus* enterocytes during sodium-coupled transport of alanine. *Biochim. Biophys. Acta* **898:**248–252

Green, R., Giebisch, G., Unwin, R., Weinstein, A.M. 1991. Coupled water transport by rat proximal tubule. *Am. J. Physiol.* **261:**F1046–F1054

Halm, D.R., Krasny, E.J., Frizzell, R.A. 1985*a*. Electrophysiology of flounder intestinal mucosa. I. Conductance properties of the cellular and paracellular pathways. *J. Gen. Physiol.* **85:**843–864

Halm, D.R., Krasny, E.J., Frizzel, R.A. 1985*b*. Electrophysiology of flounder intestinal mucosa. II. Relation of the electric potential to coupled Na-Cl absorption. *J. Gen. Physiol.* **85:**865–883

Harvey, W.R., Nedergaard, S. 1964. Sodium independent active transport of potassium in the isolated midgut of the cecropia silkworm. *Proc. Natl. Acad. Sci. USA* **51:**757–765

Hediger, M.A., Coady, M.J., Ikeda, T.S., Wright, E.M. 1987. Expression cloning and cDNA sequencing of the Na^+/glucose cotransporter. *Nature* **330:**379–381

Hill, A.E., Hill, B.S. 1978. Sucrose fluxes and junctional water flow across *Necturus* gall bladder epithelium. *Proc. R. Soc. Lond. B* **200:**163–174

Madara, J.L. 1991. Functional morphology of epithelium of the small intestine. *In:* Handbook of Physiology Sec 6, Vol. IV, pp. 83–120. American Physiological Society, Washington

Nedergaard, S., Ussing, H.H. 1997. The mechanism of isotonic water transport. *Proc. XXXIII Intern. Congr. Physiol. Sci.* PO24.07

Nielsen, S., Smith, B.L., Christensen, E.I., Agre, P. 1993. Distribution of the aquaporin CHIP in secretory and resorptive epithelia and capillary endothelia. *Proc. Natl. Acad. Sci. USA* **90:**7275–7279

Pappenheimer, J.R. 1993. On the coupling of membrane digestion with intestinal absorption of sugars and amino acids. *Am. J. Physiol.* **265:**G409–G417

Reuss, L. 1983. Basolateral KCl co-transport in a NaCl-absorbing epithelium. *Nature* **305:**723–726

Schafer, J.A. 1990. Transepithelial osmolality differences, hydraulic conductivities, and volume absorption in the proximal tubule. *Annu. Rev. Physiol.* **52:**709–726

Schultz, S.G., Curran, P.F. 1970. Coupled transport of sodium and organic solutes. *Physiol. Rev.* **50:**637–718

Schultz, S.G., Zalusky, R. 1964. Ion transport in isolated rabbit ileum. I. Short-circuit current and Na fluxes. *J. Gen. Physiol.* **47:**567–584

Spring, K.R. 1998. Routes and mechanisms of fluid transport by epithelia. *Annu. Rev. Physiol.* **60:**105–119

Sten-Knudsen, O., Ussing, H.H. 1981. The flux ratio equation under nonstationary conditions. *J. Membrane Biol.* **63:**233–242

Stirling, C.E. 1972. Radioautographic localization of sodium pump sites in rabbit intestine. *J. Cell Biol.* **53:**704–714

Sullivan, S.K., Field, M. 1991. Ion transport across mammalian small intestine. *In:* Handbook of Physiology Sect 6, Vol. IV, pp. 287–301. American Physiological Society, Washington

Sørensen, J.B., Nielsen, M.S., Nielsen, R., Larsen, E.H. 1998. Luminal ion channels involved in isotonic secretion by Na^+-recirculation in exocrine gland-acini. *Biol. Skr. Dan. Vid. Selsk.* **49:**166–178

Tse, C.M., Brant, S.R., Walker, M.S. 1992. Cloning and sequencing of a rabbit cDNA encoding an intestinal and kidney specific Na^+/H^+ exchanger isoform (NHE-3). *J. Biol. Chem.* **267:**9340–9346

Turnberg, L.F., Bieberdorf, F., Morawski, S., Fordtrand, J. 1970. Interrelationships of chloride, bicarbonate, sodium and hydrogen transport in the human ileum. *J. Clin. Invest.* **49:**557–567

Ussing, H.H. 1952. Some aspects of the application of tracers in permeability studies. *Adv. Enzym.* **XIII:**21–65

Ussing, H.H., Eskesen, K. 1989. Mechanism of isotonic water transport in glands. *Acta Physiol. Scand.* **136:**443–454

Ussing, H.H., Eskesen, K., Lim, J. 1981. The flux-ratio transient as a tool for separating transport pathways in epithelia. *In:* Epithelial Ion and Water Transport. Eds.: A.D.S. MacKnight, J.P. Leader, pp. 257–264. Raven Press, New York

Ussing, H.H., Lind, F. 1996. Trapping of $^{134}Cs^+$ in frog skin epithelium as a function of short circuit current. *Kidney Int.* **49:**1568–1569

Ussing, H.H., Lind, F., Larsen, E.H. 1996. Ion secretion and isotonic transport in frog skin glands. *J. Membrane Biol.* **152:**101–110

Ussing, H.H., Nedergaard, S. 1993. Recycling of electrolytes in small intestine of toad. *In:* Isotonic Transport in Leaky Epithelia. H.H. Ussing, J. Fischbarg, O. Sten-Knudsen, E.H. Larsen, and N.J. Willumsen. editors. *Proc. Alfred Benzon Symp.* **34:**25–34, Munksgaard, Copenhagen

Weinstein, A.M. 1988. Modeling the proximal tubule: complications of the paracellular pathway. *Am. J. Physiol.* **254:**F297–F305

Weinstein, A.M. 1992. Sodium and chloride transport. *In:* The Kidney. Physiology and Pathophysiology, 2nd edition Vol 2. D.W. Seldin, and G. Giebisch, editors. pp. 1925–1973. Raven Press, New York

Whittembury, G., De Martínez, C.V., Linares, H., Paz-Aliaga, A. 1980.

Solvent drag of large solutes indicates paracellular water flow in leaky epithelia. *Proc. R. Soc. Lond.* **B211:**63–81

Whittembury, G., Malnic, G., Mello-Aires, M., Amorena, C. 1988. Solvent-drag on sucrose during absorption indicates paracellular water flow in the rat kidney proximal tubule. *Pfluegers Arch.* **412:**541–547

Whittembury, G., Reuss, L. 1992. Mechanisms of coupling of solute and solvent transport in epithelia. *In:* The Kidney: Physiology and Pathophysiology, 2nd edition. D.W. Selding and G. Giebisch, editors. pp. 317–360. Raven Press, New York

Windhager, E.E., Whittembury, G., Oken, D.E., Schatzmann, H.J., Solomon, A.K. 1958. Single proximal tubules of the *Necturus* kidney. III. Dependence of H_2O movement on NaCl concentration. *Am. J. Physiol.* **197:**313–318

Zeuthen, T. 1995. Molecular mechanisms for passive and active transport of water. *Int. Rev. Cytol.* **160:**99–161